www.amlett.com, www.vbripress.com/aml, DOI: 10.5185/amlett.2015.5800 Published online by the VBRI Press in 2015

Nano sized C-doped TiO_2 as a visible-light photocatalyst for the degradation of 2,4,6-trichlorophenol

Atul B. Lavand, Yuvraj S. Malghe*

Department of Chemistry, The Institute of Science, 15, Madam Cama Road, Mumbai 400032, India

*Corresponding author. Tel: (+91) 22-22844219; E-mail: ymalghe@yahoo.com

Received: 10 January 2015, Revised: 29 March 2015 and Accepted: 03 April 2015

ABSTRACT

Nanosized bare and carbon (C)-doped TiO_2 were prepared using reverse micro-emulsion method. Synthesized powders were characterized with the help of X-ray diffractometer (XRD), scanning electron microscope (SEM), transmission electron microscope (TEM), energy dispersive X-ray spectroscope (EDX) and UV-visible spectrophotometer. EDX study reveals that as calcination temperature increases amount of C on TiO_2 decreases. SEM and TEM images show that TiO_2 particles are spherical in shape and after increasing the calcination temperature size of particle increases. Particle size of TiO_2 obtained from TEM data varies between 10 to 17nm. Visible light photocatalytic degradation of 2,4,6-trichlorophenol (TCP) aqueous solution was carried out using nanosized bare as well as C-doped TiO_2. UV-visible spectrophotometer and high pressure liquid chromatography (HPLC) techniques were used to analyze the concentration of TCP during the degradation process. In presence of visible light C-doped TiO_2 obtained after calcination of precursor at 300°C shows better photocatalytic activity. Parameters affecting the photocatalytic process such as calcination temperature, amount of catalyst and TCP concentration are investigated. TCP photocatalytic degradation process was optimized. It is observed that to get better photocatalytic activity optimum amount of photocatalyst and concentration of TCP solution required are 1.0 gL^{-1} and 20 mg L^{-1} respectively. Reusability study indicates that C doped TiO_2 prepared in the present work is highly stable and reusable photo catalyst. Copyright © 2015 VBRI Press.

Keywords: Visible light; C-doped TiO_2; 2,4,6-trichlorophenol; microemulsion; photodegradation.

Introduction

Special attention has been given to certain group of chemical contaminants such as chloro-organics, due to their eco-persistence. Chlorophenols constitute an array of priority chloro-organics that spell high implication in the environment [**1, 2**]. Chlorophenols are toxic compounds present in wastewater mainly arising from chemical intermediates or byproducts in petrochemical, paper making, plastic and pesticide industries. Moreover, chlorophenol is one of the most vulnerable water pollutants, which causes serious damage to the vital organs of human beings [**3, 4**]. TCP is particularly of environmental interest owing to its mutagenicity and carcinogenicity [**5**]. Uncontrolled use and disposal of TCP has led to serious impact on surface water quality [**6**]. Alarming levels of TCP were detected in several rivers from different geographical region [**7**]. Moreover, TCP is likely to form as a by-product of industrial processes such as water disinfection. Significant amount (upto 1.96 µg L^{-1}) of TCP has been detected during chlorination of drinking water [**8, 9**]. Photocatalysis is considered as one of the efficient method, used for the removal of toxic material from water [**10-13**]. This method has several advantages such as easy workup procedure, reliable results, non-toxic nature and cost-effective operation.

TiO_2 has been most widely studied photocatalyst due to its excellent stability, non-toxicity, high photo-oxidation power and low material cost. The anatase form of TiO_2 is most promising material used for degradation of water pollutants. But its major drawback is its wide band gap (~3.2 eV) which activates only under UV light irradiation. To make TiO_2 visible active it has been modified by various ways such as doping with transition metals/ non-metal, dye sensitization etc [**14-16**]. It is reported that doping of TiO_2 with non-metals such as N, S or C could help to extend the absorption wavelength from UV to visible region [**17, 18**]. Few reports about the photocatalytic degradation of TCP are available in literature [**19-21**]. In all these reports UV light is used as an irradiation source. X. Hu and co-workers reported the photocatalytic degradation of TCP in visible light using Pt nanoparticle modified rutile TiO_2 [**22**]. But this method requires costly chemicals for catalyst synthesis. In present work, we report for the first time visible light photocatalytic degradation of TCP using C doped TiO_2. Nanosized pure and C doped TiO_2 powders were synthesized using microemulsion method and used for photocatalytic activity study.

Experimental

Materials

2,4,6-trichlorophenol (TCP) obtained from S D Fine Chemicals, Mumbai and used without any further purification. Titanium isopropoxide $Ti(iOPr)_4$ was purchased from Sigma Aldrich, Mumbai and used as a source of titanium. Cyclohexane, n-butanol, N,N,N-cetyl trimethyl ammonium bromide (CTAB), acetone, and ethanol used for synthesis are AR grade and were procured from SD Fine Chemicals, Mumbai and used without further purification.

Catalyst preparation

Pure and C doped TiO_2 nanoparticles were prepared using microemulsion method. 60 mL cylclohexane, 15 mL n-butanol and 6g of *N,N,N*-acetyl trimethyl ammonium bromide were mixed and mixture was stirred for 15 min. To this microemulsion, solution containing 3 mL water and 9mL 1M titanium isopropoxide was added dropwise with constant stirring. This mixture was transferred to autoclave (with teflon-inner-liner) and kept in an oven at 150 ºC for 2h. Later it was cooled to the room temperature and the residue obtained was separated using filtration, washed several times with distilled water followed by ethanol and finally with acetone and dried at 40 ºC. The product obtained was used as a precursor. This precursor was calcined in the furnace in the temperature range 300-500 ºC for 2h.

Characterization studies

The X-ray diffraction (XRD) patterns of precursor calcined at 300, 400 and 500°C were recorded using X-ray diffractometer (XRD; Miniflex II, Rigaku) using CuKα radiation (λ= 0.15405 nm) at a scan rate 2°2θ min^{-1}. The average crystalite size of synthesized powders was calculated using Debye-Scherrer equation: $t = 0.94\lambda / \beta \cos\theta$, where t is average crystalite size, n = 0.9, β is full width of line at half maximum intensity (FWHM). The morphology and qualitative elemental analysis study of the precursor calcined at different temperatures was carried out using scanning electron microscope (SEM; 6360A, JEOL-JSM). TEM images of pure/C doped TiO_2 powder prepared in the present work were recorded using transmission electron microscope (TEM; Tecnai G^2, Philips). For TEM, sample was prepared by dispersing pure/C doped TiO_2 powder in isopropyl alcohol and solution was sonicated for 15min. The drop of solution was placed over C coated copper grid and solvent was evaporated off under IR lamp. Band gap energies of synthesized nano powders were evaluated from UV visible spectra recorded using UV visible spectrophotometer (UV/VIS; 1800, Shimadzu). This technique was also used for the estimation of amount of TCP in solution during the photocatalytic degradation process.

Measurement of photocatalytic activity

Photocatalytic activity of nanosized pure/C doped TiO_2 was tested for degradation of TCP solution. Reaction suspension was prepared by adding 0.1 g TiO_2 (obtained at 3000 °C) photo catalyst in 100 ml (20 mgL^{-1}) TCP solution. This aqueous suspension was stirred in the dark for 30min to attain adsorption-desorption equilibrium. After, the solution was irradiated with visible light. The visible light irradiation was carried out in a photo reactor using a compact fluorescent lamp (65 W, λ >420nm, Philips, Mumbai). Intensity of the light reaching to the test solution is 42 W/m^2. Temperature of test solution was maintained constant throughout the experiment by circulating water around the solution. The amount of TCP was estimated by sampling out 5ml of aliquot solution at regular time intervals. The catalyst was first separated by centrifugation, then filtered through 45 µm Millipore membrane filter and the concentration of TCP in the supernatant solution was estimated using UV-visible spectrum recorded in the wavelength range 200-400 nm. Amount of TCP in the test solution during the photocatalytic degradation process was also evaluated using HPLC technique. For this study HPLC (HPLC; 1200, Agilent) equipped with a Zobrax C-18 column (250 mm X 4.6 mm X 5 µm) with a diode array detector was used. Mobile phase used to record the chromatogram is a mixture of acetonitrile and 1% acetic acid solution in a ratio of 80:20. The injection volume of the sample used and flow rate of mobile phase are 20 µl and 1.0 $ml.min^{-1}$, respectively.

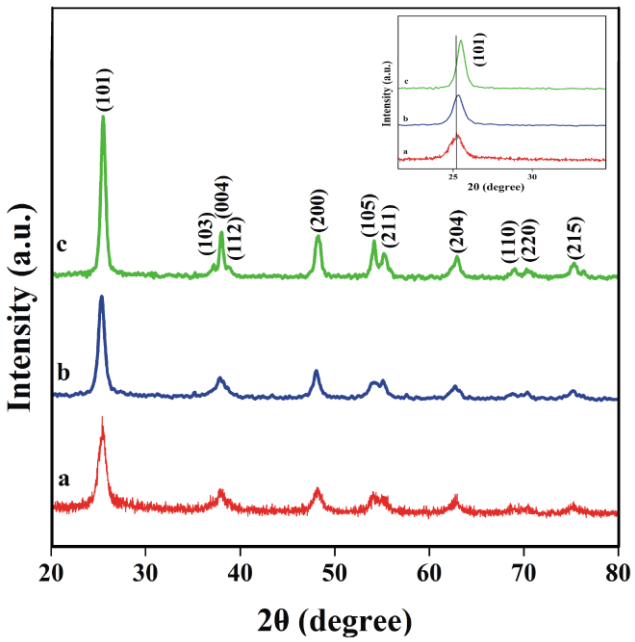

Fig. 1. XRD patterns of precursor calcined at (a) 300, (b) 400 and (c) 500°C (Inset shows the magnified view of (101) peak indicating shift in peak position.).

Results and discussion

XRD patterns of the precursor calcined at 300, 400 and 500 °C for 2 h are presented in **Fig. 1**. It is observed that TiO_2 precursor calcined at 300°C gives anatase TiO_2. Peaks at 2θ equal to 25.26, 38.16, 48.17, 54.03, 64.69, 68.16, 71.10 and 76.4° are assigned (101), (004), (200), (105), (211), (204), (110), (220), (215) hkl planes and are in good agreement with JCPD data file number 841285 (lattice planes of anatase TiO_2 phase). After increasing the calcination temperature intensity of all peaks increased due to increase in crystallinity of the product. Average

crystallite sizes of product were calculated using Debye-Scherer equation and are found between 12 to 16nm.

Effect of C doping on TiO_2 lattice parameters a, c and cell volume with respect to change in temperatures are shown in **Fig. 2a** and **b**, respectively and corresponding parameters are presented in **Table 1**.

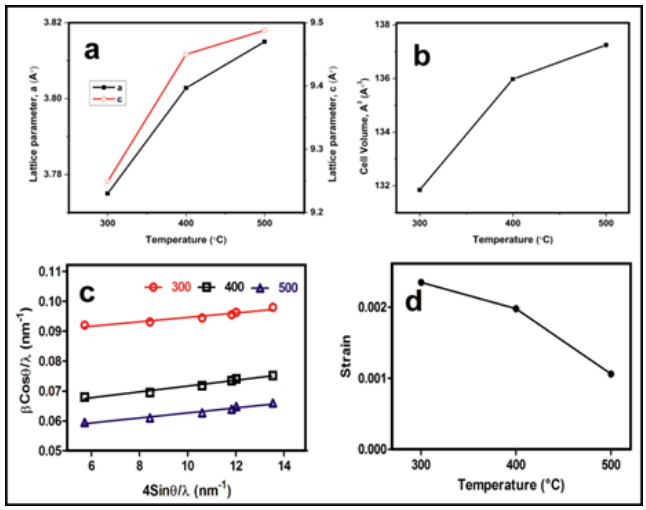

Fig. 2. (a) Variation of lattice parameters a and c with temperature, (b) change in lattice volume with respect to temperature, (c) Williamson-Hall (W-H) plot, $\beta \cos\theta/\lambda$, against 4 $\sin\theta/\lambda$ for TiO_2 and (d) variation of lattice strain with respect to temperature.

Table 1. Details of C content, lattice parameters (a and , c), lattice strain, crystallite size and band gaps of TiO_2 prepared at various temperatures.

Calcination temperature (°C)	Particle size (nm)	C content (wt%)	Lattice parameter			Lattice strain	Band gap (eV)
			a (A°)	c (A°)	Volume (A^{o3})		
300	11.4	7.59	3.775	9.249	131.85	0.002350	2.86
400	14.3	1.26	3.8028	9.45	135.98	0.001980	2.96
500	16.5	-	3.815	9.488	137.25	0.001060	3.14

As C content on TiO_2 decreases cell parameters a and c increases. With increasing calcinations temperature C content on TiO_2 decreases and (101) peak slightly shifts towards higher angle (**Fig. 1 inset**). The lattice strain induced due to C doping is determined by Williamson-Hall (W-H) equation,

$$\frac{\beta Cos\theta}{\lambda} = \frac{1}{D} + \frac{4\,\varepsilon\, Sin\theta}{\lambda}$$

Where, β is the full width at half maxima (FWHM), θ is diffraction angle, λ is X-ray wavelength, D is crystallite size and ε is lattice strain. $\frac{\beta Cos\theta}{\lambda}$ is plotted against $\frac{4\ Sin\theta}{\lambda}$ to get strain and crystallite size from slope and intercept of linear fit. **Fig. 2c**, d illustrates W-H plot and effect of lattice strain with respect to synthesis temperature for TiO_2 samples. Positive slope indicates that tensile strain is consistent with the lattice expansion. Average crystallite size and strain calculated from W-H plot for each sample is presented in **Table 1**. Sample prepared at 300°C exhibit highest lattice strain whereas TiO_2 prepared at 500°C have a lowest strain. This is due to fact that sample prepared at 300 consists doped C.

EDX spectra of precursor calcined at various temperatures were recorded and are presented in **Fig. 3 (a** and **c)**. EDX spectroscopy analysis shows that precursor calcined at 300 and 400°C contains 7.59 and 1.26% C respectively. While precursor calcined at 500°C for 2h does not contain carbon. These results reveal that after increasing the calcination temperature amount of C on TiO_2 decreases.

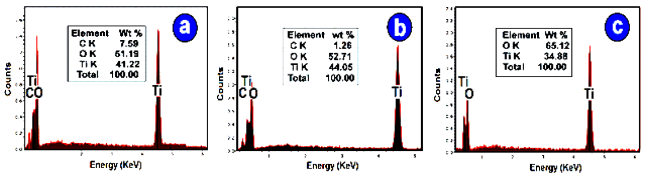

Fig. 3. EDX spectra of precursor calcined at (a) 300, (b) 400 and (c) 500 °C.

SEM images of precursor calcined at different temperatures are presented in **Fig. 4(a-c)**. These images show that at all temperatures TiO_2 particles obtained are spherical in shape. After increasing the calcination temperature grain sizes of the product increases and it also shows aggregation.

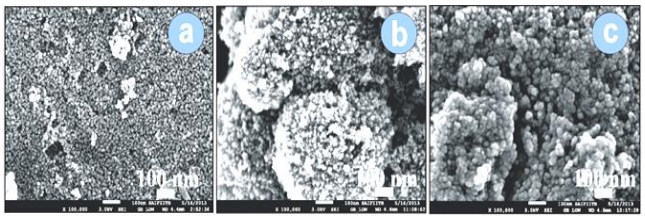

Fig. 4. FE-SEM micrographs of precursor calcined at (a) 300, (b) 400 and (c) 500°C.

TEM images of precursor calcined at different temperatures are presented in **Fig. 5 (a-c)**. TEM images show that at all temperatures TiO_2 particles obtained are spherical in shape and particle size increases with increase in temperature. Particle size of the TiO_2 obtained from TEM data varies between 10 to 17nm. Selected area electron diffraction patterns (SAED) of all the samples (inset) shows distinct rings that corresponds to the diffraction pattern of anatase TiO_2 indicating crystalline nature.

UV-visible spectra of pure and doped TiO_2 prepared at different temperatures were recorded and are presented in **Fig. 6**. Pure TiO_2 **(Fig. 6a)** exhibits the fundamental absorption edge at 396nm. This figure also shows that with increasing C content on TiO_2 its absorption wavelength increases. This distinct difference in absorption characteristic indicates that C is doped on TiO_2. The band gap energies of TiO_2 obtained at various temperatures were estimated using Tauc plot **(Fig. 7)** and are presented in **Table 1**. The band gap energies of TiO_2 obtained at 300, 400 and 500°C are 2.86, 2.96 and 3.14 eV respectively. Band gap energy of TiO_2 obtained at 300 °C is less as compared to TiO_2 obtained at 400 and 500 °C, due to this it absorbs higher wavelength light and exhibit better photocatalytic activity in visible region.

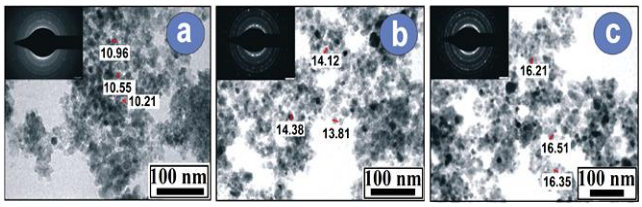

Fig. 5. TEM images of precursor calcined at (a) 300, (b) 400 and (c) 500 °C.

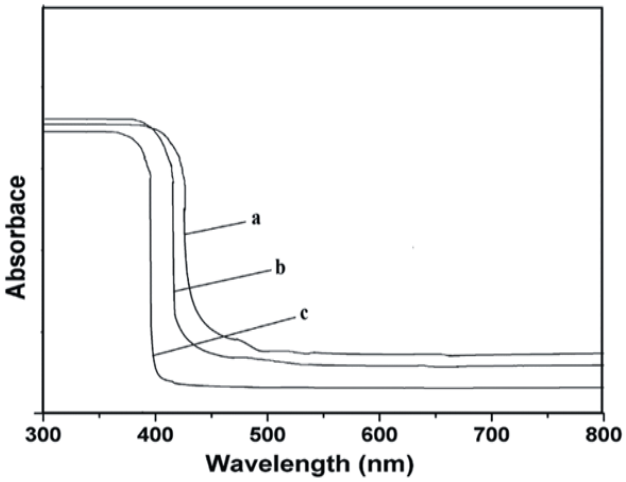

Fig. 6. UV-visible spectra of TiO_2 precursors calcined at (a) 300, (b) 400 and (c) 500 °C.

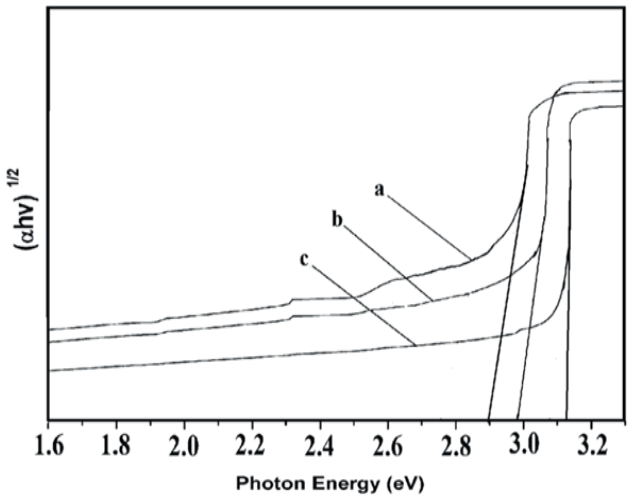

Fig. 7. Tauc plots, $(ahv)^2$ versus photon energy (hv) for TiO_2 prepared at (a) 300, (b) 400 and (c) 500 °C.

Visible light photocatalytic degradation of TCP was studied in presence of nanosized pure/C doped TiO_2 photocatalyst. Representative UV visible spectra of aqueous solution of TCP irradiated with visible light at different time intervals in presence of C doped TiO_2 (prepared at 300 °C) were recorded and are presented in **Fig. 8**. These spectra show two peaks locate at 245 and 315nm. As irradiation time increases the height of peak at both these wavelength decreases due to the photocatalytic degradation of TCP. The study indicates ~98% TCP is degraded in 90 min.

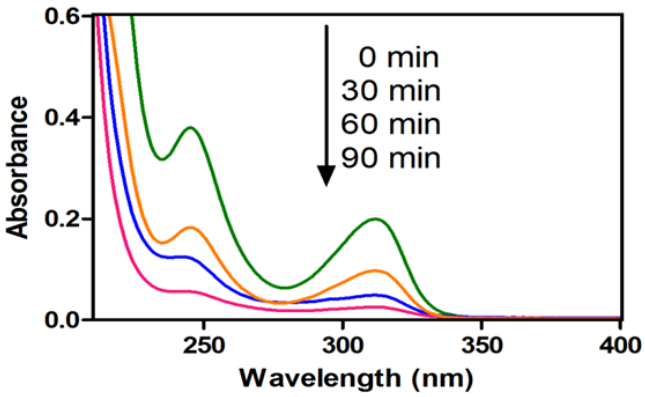

Fig. 8. UV-visible spectra of TCP solution irradiated with visible light at different time intervals in presence of C doped TiO_2 photocatalyst prepared at 300 °C

Amount of TCP in the test solution during the photocatalytic degradation process was also evaluated using HPLC technique. HPLC chromatograms of test solution irradiated at different time intervals in presence of C doped TiO_2 (prepared at 300 °C) were recorded and are presented in **Fig. 9**.

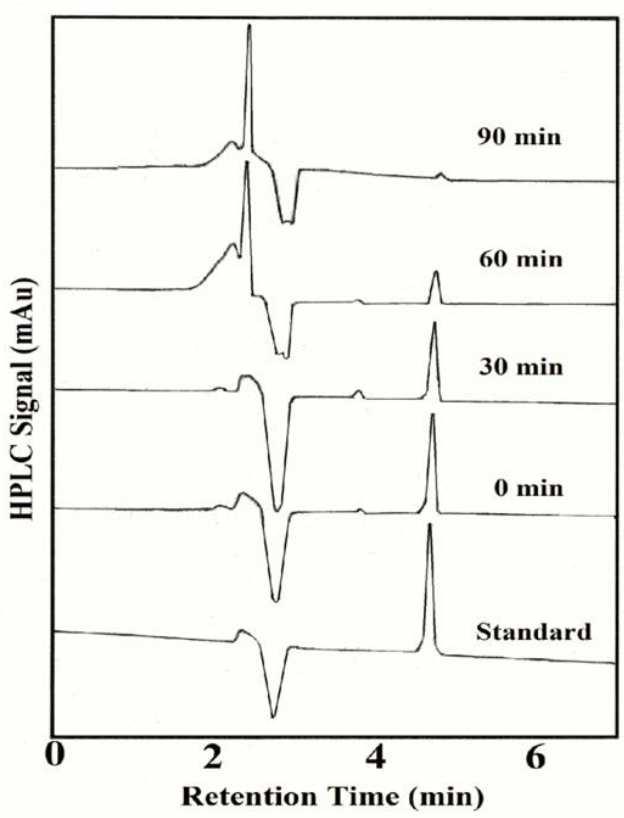

Fig. 9. HPLC chromatograms of TCP solution irradiated with visible light at different time intervals in presence of C doped TiO_2 photocatalyst prepared at 300 °C.

The chromatogram of standard solution gives two peaks at retention time 2.6 and 4.5 minutes. Peak observed at 2.6 minute is characteristic peak of water and peak at 4.5 minute is due to TCP. As irradiation time increased the intensity of peak at 4.5 min decreases, indicating that TCP degrades in visible light and ~98% mineralization occurred

in 90min. It is known that TCP degradation leads to the formation of a mixture of byproducts such as catechol, benzoquinone, resorcinol, and hydroquinone which further reacts with hydroxyl radicals and forms CO_2 and H_2O **[22-25]**. Several parameters affecting the rate of photocatalytic degradation such as calcination temperature of photocatalyst, amount of catalyst used, and concentration of TCP are explained in the following section.

Effect of calcination temperature of catalyst

TCP solution was illuminated with visible light in presence of pure and C doped TiO_2. UV-visible spectra and HPLC chromatograms of TCP solution illuminated for different time intervals were recorded and amount of TCP degraded was calculated. The plots of concentration of TCP as a function of irradiation time in presence of catalyst calcined at different temperatures are presented in **Fig. 10**. This figure shows that solution kept in dark for 30min in presence of catalyst calcined at 300, 400 and 500°C adsorbs 48, 37 and 7% TCP respectively. It is observed that as compared to pure TiO_2, C doped TiO_2 have a better adsorption efficiency this may be due to the enhancement in the adsorption of organic pollutant assisted by doped C. In absence of catalyst TCP does not degrade, which means it is stable to visible-light irradiation. Photodegradation efficiency of TiO_2 decreases with increase in the calcination temperature. As the calcination temperature increases C content on catalyst decreases. The catalyst calcined at 300°C gives better photocatalytic activity, reaching ~98% within 90min, whereas within the same period catalyst calcined at 400 and 500°C degrades only 80 and 30% TCP. This could be due to difference in size as well as C content doped on TiO_2 at different temperatures.

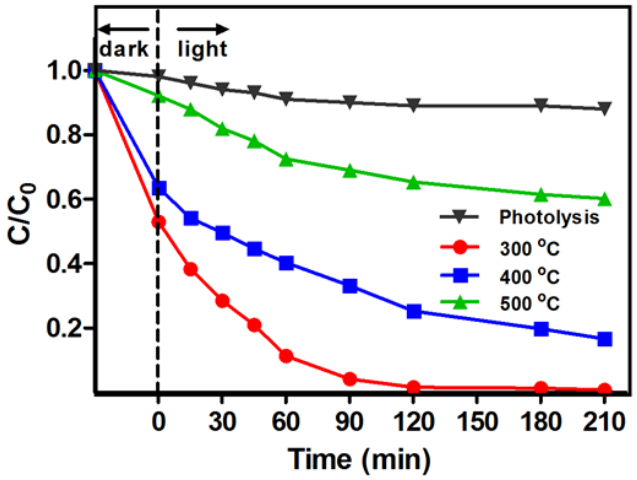

Fig. 10. Effect of calcination temperature of catalyst on photodegradation rate of TCP, catalyst calcined at (a) 300, (b) 400 and (c) 500 °C.

Effect of amount of catalyst used

Effect of amount of catalyst on photodegradation of TCP was investigated using different amount of C doped TiO_2 obtained at 300°C. For this study the amount of C doped TiO_2 was varied from 0.5 to 2.0 gL^{-1}. The concentration of TCP used to study the dose of catalyst was kept constant at 20mgL^{-1}. Photocatalytic degradation of TCP as a function of irradiation time in presence of varying amount of catalyst was investigated and the data obtained is presented in **Fig. 11**. This figure indicates that as the amount of photocatalyst in the solution increases rate of photodegradation also increases. At 1.0 gL^{-1} concentration it gives better photocatalytic activity. Further increase in the amount of photocatalyst showed decrease in the photodegradation rate. Photocatalytic degradation rate of organic pollutant depends on number of surface active sites and the photo-absorption capacity of the catalyst. If the catalyst loading is increased, rate of generation of electron/hole pairs increases which helps to increase the photodegradation rate. However, further increase in the concentration of the catalyst lead to aggregation affecting the number of active sites available for generation of electron/hole pairs. Also, high amount of catalyst loading decreases solution penetration capacity of light and hence decreases the degradation rate **[26]**.

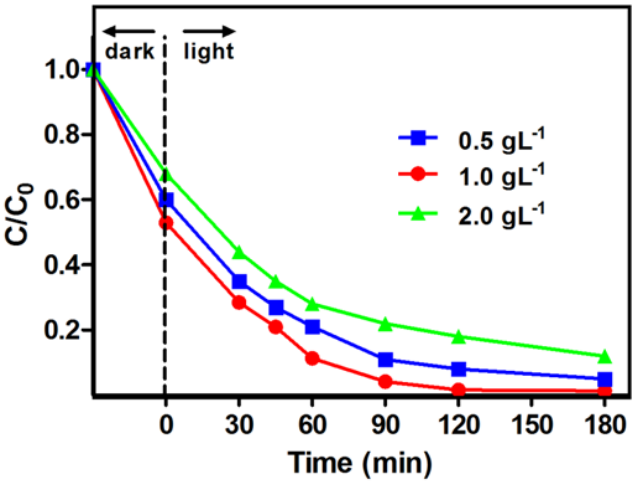

Fig. 11. Effect of catalyst loading on photodegradation rate of TCP.

Effect of initial concentration of pollutant

Effect of initial concentration on TCP photodegradation rate was studied by varying the concentrations of TCP and keeping the amount of catalyst constant (1.0gL^{-1}). Photocatalytic data obtained by varying the concentration of TCP is presented in **Fig. 12**. As seen in the figure, degradation efficiency is inversely affected by initial concentration. This is because as initial concentration of TCP increased, it get adsorbed on catalyst surface in excess amount and hinders the generation of hydroxyl radicals on that site which results in lowering the rate of photodegradation process.

Recycling of photocatalyst

C doped TiO_2 prepared at 300°C exhibit better photocatalytic activity therefore its stability was studied. Stability tests were performed by repeating the reaction three times using recovered photocatlyst. The data obtained is presented in **Fig. 13**. The data reveals that there is no noticeable decrease in photocatalytic activity up to third cycle. It indicates that C doped TiO_2 prepared in the present work is highly stable and reusable photocatalyst.

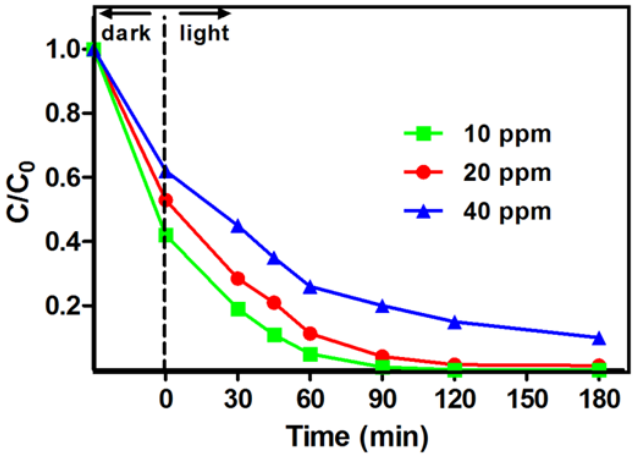

Fig. 12. Effect of initial concentration of TCP on the photodegradation rate.

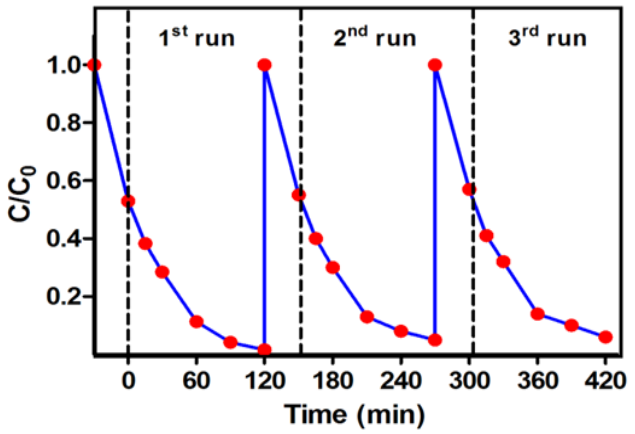

Fig. 13. Reuse of photocatalyst up to third cycle.

Conclusion

1. Nanosized Pure as well as C doped TiO_2 photocatalysts were synthesized using microemulsion method.
2. C doped TiO_2 show red-shift in absorption spectra attributed to significant enhancement in its photo absorption capacity for visible light.
3. Photocatalytic activity depends on C doping as the amount of C in TiO_2 increases the photocataltic activity also increases.
4. TCP photocatalytic degradation process was optimized and it is concluded that C doped TiO_2 prepared at 300°C exhibit better photocatalytic activity. Also, to get better photocatalytic activity optimum amount of photocatalyst and concentration of TCP solution required are 1.0 gL^{-1} and 20mg L^{-1} respectively.
5. Photocatalytic efficiency does not change up to third cycle and catalyst is quiet stable.

Acknowledgements

Authors are thankful to SAIF, IIT, Mumbai, India for recording the FE-SEM and TEM images of sample. One of the author Atul B. Lavand is grateful to UGC, New Delhi, India for providing BSR fellowship.

Reference

1. Yin, D.; Hu, S.; Jin, H.; Yu, L.; *Chemosphere*, **2003**, *52* , 67. **DOI:** 10.1016/S0045-6535(03)00273-X
2. Krijgsheld, K.R.; Van der Gen, A.; *Chemosphere*, **1986**, *15*, 825. **DOI:** 10.1016/0045-6535(86)90051-2
3. D'Olivera, J.C.; Al-sayed, G.; Pichat, P.; *Environ. Sci. Technol.*, **1990**, *24*, 990. **DOI:** 10.1021/es00077a007
4. Keith, L.H.; Telliard, W.A.; *Environ. Sci. Technol*., **1979**, *13*, 416. **DOI:** 10.1021/es60152a601
5. Lewis, R.J.; Sr, R.J.; Hazardous Chemicals Desk Reference; 5 th edn. John Wiley and Sons, New York, **2002**.
6. U. S. Environmental protection Agency, Superfund, Record of Decision: Ohio River Park America (EPA- PAD980508816 OU03, **1998**.
7. Gao, J.; Liu, L.; Liu, X.; Zhou, H.; Huang, S.; Wang, Z.; *Chemosphere*, **2008**, *7*, 1181. **DOI:** 10.1016/j.chemosphere.2007.10.018
8. Nikolaou, A.D.; Kostopoulou, M.N.; Lekkas, T.D.; *Global Nest Int. J.*, **1999**, *1*, 143.
9. Fingler, S., Drevenkar, V.; *Toxicol. Environ. Chem.*, **1988**, *17*, 319. **DOI:** 10.1080/02772248809357298
10. Hoffmann, M.R.; Martin, S.T.; Choi, W.Y.; Bahnemann, D.W.; *Chem. Rev.*, **1995**, *95*, 69. **DOI:** 10.1021/cr00033a004
11. Kant S.; Kumar, A.; *Adv. Mat. Lett*., **2012**, *3*(4), 350. **DOI:** 10.5185/amlett.2012.5344
12. Muthirulan P.; Devi, C.K.N.; Sundaram, M.M.; *Adv. Mat. Lett*., **2014**, *5*(4), 163. **DOI:** 10.5185/amlett.201 3.7507
13. Kuriakose S.; Satpati, B.; Mohapatra, S.; *Adv. Mat. Lett*., **2015**, *6*(3), 217. **DOI:** 10.5185/amlett.201 5.5693
14. Kish, H., Zang, L., Lange, C., Maier, W.F.; Antonius, C.; Meissner, D.; *Angew. Chem*., **1998**, *37*, 3034.
15. Wang, C.; Bahnemann, D.W.; Dohrmann, J.K.; *Chem. Commun.*, **2000**, *16*, 1539. **DOI:** 10.1039/B002988M
16. Bae, E.; Choi, W.; Park, J.; Shin, H.S.; Kim, S.B.; Lee, J.S.; *J. Phys. Chem. B*, **2004**, *108*, 14093. **DOI:** 10.1021/jp047777p
17. Livraghi, S.; Paganini, M.C.; Giamello, E.; Selloni, A.; Valentin, C.D.; Pacchioni, G.; *J. Am. Chem. Soc*., **2006**, *128*, 15666. **DOI:** 10.1021/ja064164c
18. Valentin, C.D.; Pacchioni, G.; Selloni, A.; *Chem. Mater*., **2005**, *17*, 6656. **DOI:** 10.1021/cm051921h
19. Rengaraj, S.; Li, X.Z.; *J. Mol. Catal. A: Chem*., **2006**, *243*, 60. **DOI:** 10.1016/j.molcata.2005.08.010
20. Anandan, S.; Vinu, A.; Mori, T.; Gokulakrishnan, N.; *Catal. Comm*., **2007**, *8*, 1377. **DOI:** 10.1016/j.catcom.2006.12.001
21. Gaya, U.I.; Abdullah, A.H.; Hussein, M.Z.; Zainal, Z.; *Desalination*, **2010**, *263*, 176. **DOI:** 10.1016/j.desal.2010.06.055
22. Hu, X.; Ji, H.; Wu, L.; *RSC Adv*., **2012**, *2*, 12378. **DOI:** 10.1039/C2RA21661B
23. Aal, A.A.; Mahmoud, S.A.; *Nanoscale Res. Lett*., **2009**, *4*, 627. **DOI:** 10.1007/s11671-009-9290-1
24. Ahmed, S.; Rasul, G.M.; Martens, N.W.; Brown, R.; Hasib, A.M.; *Water air soil poll*., **2011**, *215*, 3. **DOI:** 10.1007%2Fs11270-010-0456-3
25. Selvam, N.C.; Narayanan, S.; Kennedy, L.J.; Vijaya, J.J.; *J. Environ. Sci*., **2013**, *25*, 2157. **DOI:** 10.1016/S1001-0742(12)60277-0
26. Fox, M.A.; Dulay, M.T.; *Chem. Rev*., **1993**, *93*, 341. **DOI:** 10.1021/cr00017a016